ISSN 0915-633X

NATIONAL INSTITUTE FOR FUSION SCIENCE

Integrated ELM Simulation with Edge MHD Stability and Transport of SOL-divertor Plasmas

N. Hayashi, T. Takizuka, N. Aibe, T. Ozeki, N. Oyama

(Received - June 12, 2007)

NIFS-876 July 2007

RESEARCH REPORT
NIFS Series

TOKI, JAPAN

Integrated ELM simulation with edge MHD stability and transport of SOL-divertor plasmas

N. Hayashi, T. Takizuka, N. Aiba, T. Ozeki, N. Oyama

Japan Atomic Energy Agency, Naka, Ibaraki-ken, 311-0193 Japan

Abstract The effect of the pressure profile on the energy loss caused by edge localized modes (ELMs) has been investigated by using an integrated simulation code TOPICS-IB based on a core transport code with a stability code for the peeling-ballooning modes and a transport model for scrape-off-layer and divertor plasmas. The steep pressure gradient inside the pedestal top is found to broaden the region of the ELM enhanced transport through the broadening of eigenfunctions and enhance the ELM energy loss. The ELM energy loss in the simulation becomes larger than 15 % of the pedestal energy, as is shown in the database of multi-machine experiments.

Keywords: ELM, MHD stability, SOL-divertor plasmas, integrated simulation

1 Introduction

Edge localized modes (ELMs) are indispensable to sustain a H-mode plasma. The ELMs, however, induce sometimes very large heat load on divertor plates and cause the reduction of the plate lifetime in tokamaks. The ELMs are considered to be induced by the high-n ballooning mode due to the large pressure gradient or by the medium-n peeling mode due to the large edge current and the pressure gradient. ELM characteristics, such as the energy loss, the collapse structure and so on, have been measured experimentally with a high resolution of time and space [1-4]. Analyses of the ELMs from multi-machine experiments has shown that the ELM energy loss increases with decreasing the collisionality and becomes larger than 15 % of the pedestal energy [2]. Although effects of the bootstrap current and the scrape-off-layer (SOL) transport on the ELM energy loss have been discussed [2,3], the physical understanding and the quantitative evaluation are not fully accomplished so far. It is necessary to clarify the physical mechanism of the ELM energy loss and its collisionality dependence for the projection in the ITER and fusion reactors.

The modeling of various physics elements and the integration of those models are a useful and effective method to simulate complex plasmas with various time and spatial scales. This integrated code is one of the effective tools to study the self-consistent ELM behavior [5-8], while the nonlinear simulation [9,10] is a fundamental method requiring large computational resources. The integrated codes couple with ELM models, which consists of the edge transport and the stability. Previous codes dealt with the ELM behavior without the dynamic response of SOL-divertor plasmas. The SOL-divertor plasmas, however, play important roles in the ELM behavior by changing boundary conditions of the pedestal transport. Indeed, the edge boundary conditions at the separatrix were found to affect the ELM behavior in the integrated simulation [6]. An appropriate SOL-divertor model is required for the integrated code.

A two-point model based on integral fluid equations can reproduce fairly well static features of SOL-divertor plasmas in experiments with a very short computation-time [11]. Such point models are suitable for coupling with core transport codes [12]. We have extended the point model and developed a dynamic five-point model to study the response of the SOL-divertor plasmas to an ELM crash [13]. This five-point model

can reproduce well static and dynamic features obtained by particle and fluid codes.

From these points of view, we have developed an integrated code TOPICS-IB [14] with the five-point model [13] and a stability code for peeling-ballooning modes, MARG2D [15]. The TOPICS-IB is based on a 1.5-dimensional (1.5D) core transport code TOPICS [16] extended to the integrated simulation for burning plasmas. TOPICS-IB successfully simulates a series of transient behaviors of an H-mode plasma; the pedestal growth, an ELM crash and the recovery of the pedestal. The collisionality dependence of the ELM energy loss was found to be caused by both the edge bootstrap current and the SOL transport parallel to the magnetic field. The collisionality dependence caused by the parallel transport was also pointed out by the analytical model [17]. In the previous simulation, however, the ELM energy loss was less than 10 % of the pedestal energy because the mode structure was localized in a pedestal region with a steep pressure gradient [14].

In this paper, we study effects of pressure profile on the ELM energy loss by using the TOPICS-IB. In experiments [1-4,18], the pressure gradient inside the pedestal top varies. The different pressure gradient inside the pedestal top may broaden the mode structure and enhance the ELM energy loss. The resultant ELM energy loss is compared with that in experiments. For the ELM energy loss enhanced by the different pressure gradient inside the pedestal top, we again investigate the collisionality dependence of the ELM energy loss by artificially enhancing the collisionality in the bootstrap current and SOL-divertor models. In the next section, we explain details of the TOPICS-IB. Simulation results are shown in Section 3. Summary and discussion are given in Section 4.

2 Integrated code TOPICS-IB for the ELM dynamics

The ELM energy loss is investigated by the TOPICS-IB, in which the TOPICS is coupled with the ELM model [5] and the SOL-divertor model [13]. Details of the TOPICS-IB are shown in [14] and some essential features are explained as follows.

The TOPICS self-consistently solves the 1D transport and current diffusion equations and the Grad-Shafranov equation of the MHD equilibrium on the 2D plane. The transport equations are the continuity equation for the deuterium ion density, n_i, the

power balance equations for the electron temperature, T_e, and the ion temperature, T_i, on the coordinate of the normalized minor radius, ρ, defined by the square root of the toroidal flux. In this paper, thermal diffusivities are assumed as $\chi_{e,i} = \chi_{neo,i} + \chi_{ano,e,i}$, where $\chi_{neo,i}$ denotes the neoclassical ion diffusivity calculated by the matrix inversion method [19], which also calculates the bootstrap current. The anomalous diffusivities $\chi_{ano,e,i}$ are simply given as an empirical formula, $\chi_{ano,e} = 0.18\ (1+2\rho^3)\ (1+P_{NB}^{0.5})\ m^2/s$ and $\chi_{ano,i} = 2\ \chi_{ano,e}$, where P_{NB} is the neutral beam power in the unit of MW. In order to produce the H-mode pedestal structure, the transport near the edge is reduced to the neoclassical level ($\chi_{ano,e,i}=0$) as shown in a case with a solid line in Fig.1(a). The region of the reduced transport is prescribed for simplicity so that the pedestal width, Δ_{ped}, is fixed constant. Additionally, in order to steepen the pressure gradient inside the pedestal top, the transport is reduced step by step in a given region inside the pedestal top as shown in cases with lines except for the solid one in Fig.1(a).

The ELM model [5] has been developed by coupling the TOPICS with a linear MHD stability code MARG2D [15]. In the present simulation, stabilities of n=1-30 modes are examined by the MARG2D at given time-intervals along the pedestal growth, where n is the toroidal mode number. When some modes become unstable, an ELM is assumed to occur. The diffusivity is assumed to be enhanced according to radial profiles of eigenfunctions of unstable modes as follows: $\chi_{e,i} = \chi_{neo,i} + \chi_{ano,e,i} + \chi_{ELM}$. The ELM enhanced diffusivity χ_{ELM} is $\chi_{ELM} = \chi_{ELM}^{max} \times (\Sigma_n\ \xi_{r,n}^2)/N$, where χ_{ELM}^{max} is the maximum value, $\xi_{r,n}$ denote the radial displacement of the plasma by the unstable mode with specific n, and N is the total number of the unstable modes with various n. The profile of the radial displacement $\xi_{r,n}$ is assumed to be the sum of poloidal mode components of the eigenfunction, $\xi_{r,n,m}$, i.e., $\xi_{r,n} \propto \Sigma_m\ \xi_{r,n,m}$, where $\xi_{r,n}$ is normalized by its maximum value. The ELM enhanced transport is maintained for a time interval τ_{ELM} given as a parameter.

We couple the five-point model [13] to the TOPICS for a self-consistent transport covering core-pedestal-SOL-divertor plasmas. The five-point model is based on the integral of time dependent fluid equations, i.e., particle, momentum, electron and ion temperatures, generalized Ohm's law and current equations. The model geometry is an

open magnetic flux-tube nearest to the separatrix. The flux tube is divided into four regions: the SOL region divided into two regions at the stagnation point where the parallel particle flux is zero and two divertor regions on either side of the SOL region. The integral fluid equations in each region are reduced to a set of nonlinear equations with physical variables at five positions (stagnation point, upstream throats of divertor regions and sheath entrances). Exponential radial profiles are assumed and those characteristic scale length are solved. A kinetic-effect model (heat flux limit) based on results from the particle code is introduced. The five-point model can deal with the in-out/up-down asymmetry of divertor plasmas, but the symmetry is assumed in this paper for simplicity. Heat and particle diffusivities in the five-point model are set equal to those values at the separatrix in the TOPICS. The localization of ELMs at the low-field side midplane and the filamentary structure [9,20] are not taken into account in the present model, as the same in other integrated codes [6-8]. The collisionality dependence in the five-point model appears through the parallel heat conduction and the equipartition energy flow between electrons and ions.

3 Simulation results

The ELM activity is simulated for JT-60U like parameters: R=3.4 m, a=0.9 m, κ=1.5, δ=0.21, I_p=1.8 MA, B_t=3.5 T, q_{95}=3.8 and β_N~0.8-1.7. The ELM parameters are chosen as τ_{ELM}=400 μs, χ_{ELM}^{max}=200 m^2/s and Δ_{ped}=0.05. Experimental analyses suggested that the collisionality dependence of the ELM energy loss is mainly caused by the collapse of the temperature profile during an ELM crash and the collapse of the density profile has a little influence on the collisionality dependence [2-4]. Therefore, in this paper, we solve the temperature profile and fix the density one as $n_i = 3.6 \times 10^{19} (0.8\ (1-\rho^2)^{0.5} + 0.2)\ m^{-3}$ ($n_{iSOL} = 7.2 \times 10^{18}\ m^{-3}$), for simplicity. The divertor plasma is assumed to be under the high recycling condition and the divertor plasma density, n_{idiv}, is chosen as $n_{idiv}=1\times10^{20}\ m^{-3}$.

Figure 1(a) shows χ_e profiles where the transport is reduced to the neoclassical level in a given region with $0.87<\rho<1$ for the pedestal in a case A and the transport is additionally reduced step by step in a given region with $0.75<\rho<0.94$ in other cases

from B to D. Figure 1(b) shows the time evolution of T_e profile in the case A. Along the time evolution, the pedestal grows and temperature increase in core and pedestal regions. In the progress of the pedestal growth, high-n modes (n>10) become unstable and an ELM occurs. Figure 2(a) shows profiles of the total pressure, P, at the ELM onset in the same cases from A to D as in Fig.1(a). In Fig.2(a), the pedestal top is located at ρ=0.925 in all cases and the pressure gradient inside the pedestal top becomes steep in order of A, B, C, D. Even the pressure gradient inside the pedestal top in the case A is a little larger than those observed in JT-60U [1,18]. While the pressure gradients inside the pedestal top are different, pedestal gradients ρ=0.95 are almost the same at the ELM onset. In all cases in Fig.2, plasma parameters at the pedestal top are T_{eped}~2.1 keV, T_{iped}~2.4 keV and the normalized electron collisionality, $\nu^*_{ped0}=\pi R q_{95}/\lambda_{ee}=0.06$, where λ_{ee} is the electron mean free path.

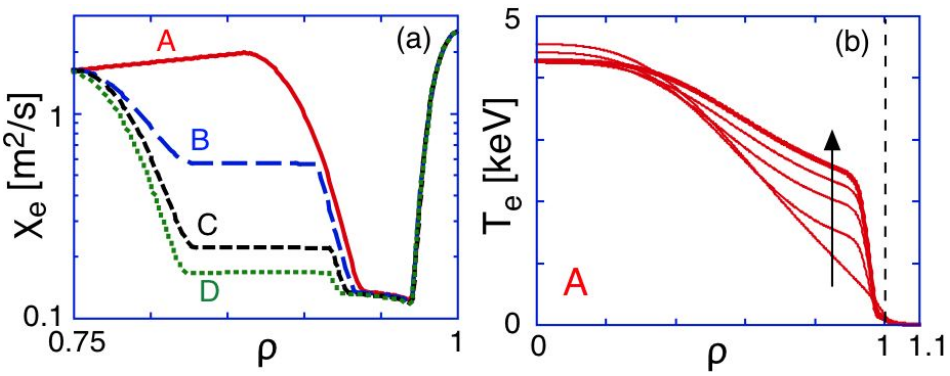

Fig. 1 (a) χ_e profiles in each case from A to D and (b) time evolution of T_e profile in case A (20 ms interval) before ELM. In (b), separatrix is located at ρ=1 and SOL is a region with ρ > 1.

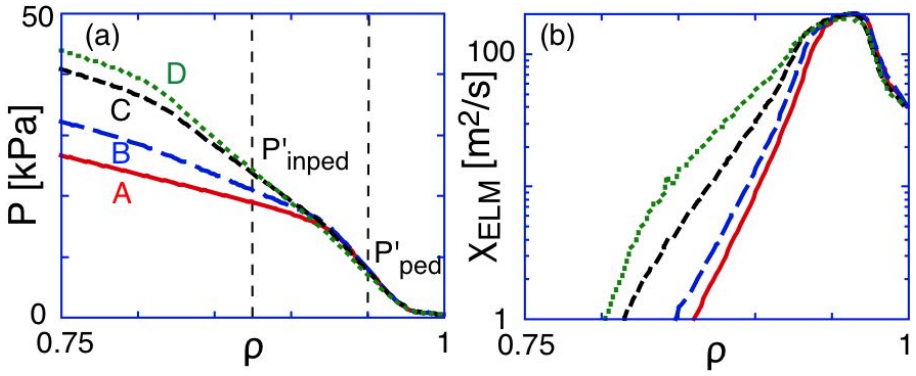

Fig. 2 Profiles of (a) P at ELM onset and (b) χ_{ELM} in each case from A to D. In (a), pressure gradients, P'_{inped} and P'_{ped}, are defined and used in Fig.4.

Figure 2(b) shows χ_{ELM} profiles in the cases from A to D. In the case A, the unstable mode structure is localized in the pedestal region with a steep pressure gradient. The steep pressure gradient broaden the eigenfunctions and the region of the ELM enhanced transport in the cases B-D. Figure 3 shows the time evolution of T_e profile during the ELM in (a) case A and (b) C. The collapse of the temperature profile occurs in the pedestal region and deeply inside the pedestal region. When an ELM crash occurs, the SOL plasma temperature at ρ=1 rapidly increases due to the energy flow from the pedestal to the SOL in Fig.3. The increase of the SOL temperature mitigates the radial edge gradient and lowers the ELM energy loss. As the region of the ELM enhanced transport is broadened in Fig.2(b), the collapse becomes large (Compare Fig.3(a) with Fig.3(b)) and the ELM energy loss becomes large as discussed below.

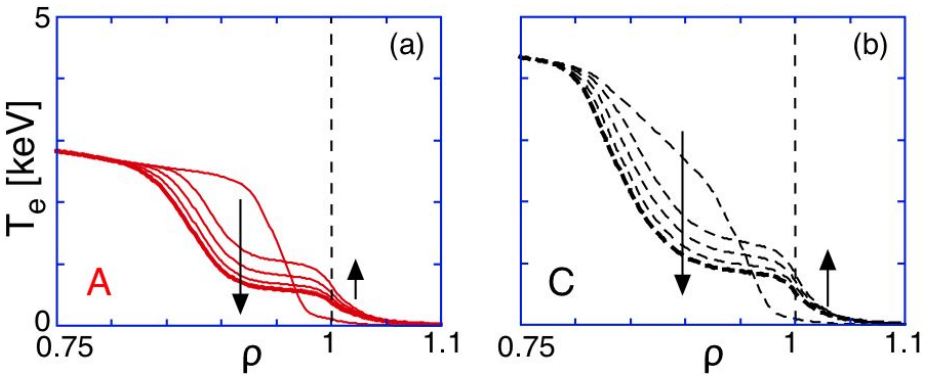

Fig. 3 Time evolution of T_e profile in (a) case A and (b) case C (100 μs interval) during ELM.

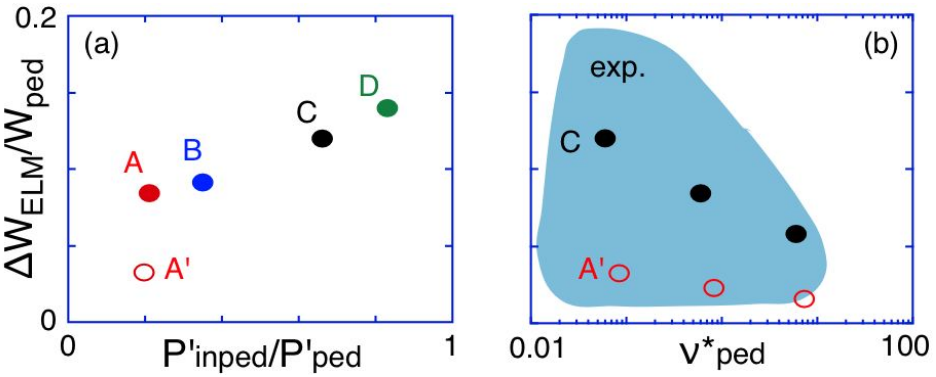

Fig. 4 (a) $\Delta W_{ELM}/W_{ped}$ versus P'_{inped}/P'_{ped} for ν^*_{ped}=0.06 (A-D) and (b) $\Delta W_{ELM}/W_{ped}$ versus ν^*_{ped} for P'_{inped}/P'_{ped}=0.66 (C). Results in previous study [14] are shown by open symbols A'. In (b), shaded region denotes experimental data [1,2].

Figure 4(a) shows the magnitude of the ELM energy loss, ΔW_{ELM}, normalized the pedestal energy, W_{ped}~1.5 MJ, as a function of P'_{inped}/P'_{ped} where P'_{inped} and P'_{ped} denote $P'=dP/d\rho$ at $\rho=0.875$ and 0.95, respectively, as defined in Fig.2(a). In the case A with $P'_{inped}/P'_{ped}=0.21$, the ELM energy loss is less than 10 % of the pedestal energy and is comparable with those in JT-60U [1]. As a reference, we add a result in the previous study [14], which indicated by A' in Fig.4. In the case A', values of τ_{ELM} and χ_{ELM}^{max} are reduced half to τ_{ELM}=200 μs and χ_{ELM}^{max}=100 m^2/s, and the plasma current is reduced to I_p=1.5 MA (q_{95}=4.6). As mentioned in Ref.[14], the ELM energy loss is enhanced by increasing the values of τ_{ELM} and χ_{ELM}^{max}. The lowering of q_{95} also enhances the ELM energy loss. These variations of τ_{ELM}, χ_{ELM}^{max} and q_{95} are not enough for $\Delta W_{ELM}/W_{ped}$ > 0.1 with P'_{inped}/P'_{ped}~0.2. As shown in Fig.4(a), the steep pressure gradient inside the pedestal top enhances the ELM energy loss. The density collapse, which is not considered in this paper, enhances the values of $\Delta W_{ELM}/W_{ped}$ by about 50 % under the assumption of the similar collapse to the temperature one. For example, the density collapse enhances the value of $\Delta W_{ELM}/W_{ped}$ from 0.12 to 0.18 in the case C. The ELM energy loss in the simulation becomes larger than 15 % of the pedestal energy, as is shown in the database of multi-machine experiments with the low collisionality (ν^*_{ped}<0.1) [2].

For the case C in Figs 1-3, we investigate the collisionality dependence by artificially enhancing the collisionality in both bootstrap current and SOL-divertor models. As found in Ref.[14], for the high collisionality, the bootstrap current reduces the region of the ELM enhanced transport through the profile modification of the magnetic shear and eigenfunctions of unstable modes. On the other hand, the parallel heat conduction in the SOL transport decreases with increasing the collisionality, which results in the further increase of the SOL temperature. These two effects reduce the ELM energy loss for the high-collisional plasma. Figure 4(b) shows the dependence of $\Delta W_{ELM}/W_{ped}$ on an artificially enhanced collisionality, $\nu^*_{ped}=C_e\nu^*_{ped0}$, for C_e=1, 10, 100 where C_e is an enhancing factor in the models. When the collisionality is enhanced by C_e=100 (ν^*_{ped}=6), the total energy loss is reduced about half. This half reduction is almost the same as in the previous study [14] shown by A' in Fig.4(b). Although the magnitude of the ELM energy loss is changed by the pressure gradient inside the

pedestal top in Fig.4(a), the collisionality dependence of the ELM energy loss through the bootstrap current and the SOL transport in Fig.4(b) is unchanged. In Fig.4(b), the half reduction in the simulation is a little small compared with experiments [2], in which the ELM energy loss is reduced by about 1/3. The collisionality dependence of the pressure gradient inside the pedestal top possibly enhances the reduction.

4 Summary and discussion

We have investigated the effect of the pressure profile on the ELM energy loss by using an integrated simulation code TOPICS-IB. The steep pressure gradient inside the pedestal top is found to broaden the region of the ELM enhanced transport through the broadening of eigenfunctions and enhance the ELM energy loss. The ELM energy loss in the simulation becomes larger than 15 % of the pedestal energy, as is shown in the database of multi-machine experiments [2]. Although the magnitude of the ELM energy loss is changed by the pressure profile, the collisionality dependence of the ELM energy loss through the bootstrap current and the SOL transport found in the previous study [14] is unchanged. The collisionality dependence of the pressure gradient inside the pedestal top possibly enhances that of the ELM energy loss.

In order to validate our models, simulations for various tokamaks and comparisons with experiments and nonlinear simulations are our future works. The model improvement, such as the density dynamics, the transport model which determines the pressure gradient inside the pedestal top as well as the pedestal width, and so on, is necessary. The dynamics of the pedestal density strongly connects with the neutral recycling. The integration of neutral models in both the TOPICS and the SOL-divertor model is in progress.

Acknowledgements

We would like to thank Dr. R. Hiwatari for fruitful discussion and comments and Mr. I. Kamata for developing and running the integrated code. We are grateful to JT-60 team members for collaboration. This work was partly supported by JSPS, Grant-in-Aid for Scientific Research. This work was also carried out under the collaborating research program at National Institute for Fusion Science (NIFS06 KDBI001). We would like to

thank Drs A. Takayama and Y. Tomita for taking care of the NIFS program.

References

[1] N. Oyama, et al., Nucl. Fusion **44**, 582 (2004).

[2] A. Loarte, et al., Plasma Phys. Control. Fusion **45**, 1549 (2003).

[3] A.W. Leonard, et al., J. Nucl. Mater. **313-316**, 768 (2003).

[4] M.R. Wade, et al., Phys. Plasmas **12**, 056120 (2005).

[5] T. Ozeki, et al., Fusion Sci. Tech. **50**, 68 (2006).

[6] T. Onjun, et al., Phys. Plasmas **12**, 012506 (2005).

[7] J.S. Lonnroth, et al., Contrib. Plasma Phys. **46**, 726 (2006).

[8] A.Y. Pankin, et al., Nucl. Fusion **46**, 403 (2006).

[9] P.B. Snyder, et al., Phys. Plasmas **12**, 056115 (2005).

[10] P. Beyer, et al., Phys. Rev. Lett. **94**, 105001 (2005).

[11] P.C. Stangeby, The plasma boundary of magnetic fusion devices, Institute of physics publishing, Bristol and Philadelphia, 2000.

[12] R. Hiwatari, et al., J. Nucl. Mater. **337-339**, 386 (2005).

[13] N. Hayashi, et al., J. Nucl. Mater. **363-365**, 1044 (2007).

[14] N. Hayashi, et al., "Integrated simulation of ELM energy loss determined by pedestal MHD and SOL transport", in Proc. 21th IAEA FEC 2006 (Chengdu) CD-ROM file TH/4-2, to be published in Nucl. Fusion.

[15] N. Aiba, et al., Nucl. Fusion **47**, 297 (2007).

[16] N. Hayashi, et al., J. Plasma Fusion Res. **80**, 605 (2004).

[17] M.Z. Tokar, et al., Plasma Phys. Control. Fusion **49**, 395 (2007).

[18] H. Shirai, et al., Plasma Phys. Control. Fusion **42**, 1193 (2000).

[19] M. Kikuchi, et al., Nucl. Fusion **30**, 343 (1990).

[20] A. Kirk, et al. Phys. Rev. Lett. **92**, 245002 (2004).